

# Sleep Homeostasis and Cortical Synchronization: II. A Local Field Potential Study of Sleep Slow Waves in the Rat

Vladyslav V. Vyazovskiy, PhD<sup>1</sup>; Brady A. Riedner, BS<sup>1-3</sup>; Chiara Cirelli, MD PhD<sup>1</sup>; Giulio Tononi, MD PhD<sup>1</sup>

<sup>1</sup>Department of Psychiatry, <sup>2</sup>Neuroscience Training Program, <sup>3</sup>Clinical Neuroengineering Training Program, University of Wisconsin, Madison, WI

**Study Objective:** Sleep slow-wave activity (SWA, EEG power between 0.5 and 4.0 Hz) decreases homeostatically in the course of non-rapid eye movement sleep (NREM) sleep. According to a recent hypothesis, the homeostatic decrease of sleep SWA is due to a progressive decrease in the strength of corticocortical connections. This hypothesis was evaluated in a large-scale thalamocortical model, which showed that a decrease in synaptic strength, implemented through a reduction of postsynaptic currents, resulted in lower sleep SWA in simulated local field potentials (LFP). The decrease in SWA was associated with a decreased proportion of high-amplitude slow waves, a decreased slope of the slow waves, and an increase in the number of multipeak waves. Here we tested the model predictions by obtaining LFP recordings from the rat cerebral cortex and comparing conditions of high homeostatic sleep pressure (early sleep) and low homeostatic sleep pressure (late sleep).

**Design:** Intracortical LFP recordings during baseline sleep and after 6 hours of sleep deprivation.

**Setting:** Basic sleep research laboratory.

**Patients or Participants:** WKY adult male rats.

**Interventions:** N/A.

**Measurements and Results:** Early sleep (sleep at the beginning of the major sleep phase, sleep immediately after sleep deprivation) was associated with (1) high SWA, (2) many large slow waves, (3) steep slope of slow waves, and (4) rare occurrence of multipeak waves. By contrast, late sleep (sleep at the end of the major sleep phase, sleep several hours after the end of sleep deprivation) was associated with (1) low SWA, (2) few high-amplitude slow waves, (3) reduced slope of slow waves, and (4) more frequent multipeak waves.

**Conclusion:** In rats, changes in sleep SWA are associated with changes in the amplitude and slope of slow waves, and in the number of multipeak waves. Such changes in slow-wave parameters are compatible with the hypothesis that average synaptic strength decreases in the course of sleep.

**Keywords:** sleep homeostasis, sleep regulation, EEG, rat, period-amplitude analysis

**Citation:** Vyazovskiy VV; Riedner BA; Cirelli C; Tononi GT. Sleep homeostasis and cortical synchronization: II. A local field potential study of sleep slow waves in the rat. *SLEEP* 2007;30(12):1631-1642.

IN MOST SPECIES, SLEEP PRESSURE INCREASES AS A FUNCTION OF THE TIME SPENT AWAKE AND DECREASES IN THE COURSE OF SLEEP, INDICATING THAT SLEEP is homeostatically regulated. There are several markers of sleep pressure, which reflect the fact that both the duration and the intensity of sleep are under homeostatic control.<sup>1</sup> The best characterized physiological indicator of sleep intensity is the level of electroencephalogram (EEG) slow-wave activity (SWA, EEG power between 0.5 and 4.0 Hz) during non-rapid eye movement (NREM) sleep (<sup>2,3</sup>, reviewed in<sup>1</sup>). In mammals, sleep SWA is high in early sleep, when sleep pressure is high, and decreases progressively to reach low levels in late sleep.<sup>4-9</sup> Moreover, sleep SWA increases further with sleep deprivation, and is reduced by naps.<sup>1,9</sup> While in many cases sleep intensity and sleep duration change in parallel, SWA can increase or decrease without changes in sleep duration.<sup>1,9</sup>

The EEG power in the SWA range reflects synchronous oscillations of large populations of cortical neurons, which can be recorded as low-frequency waves in intracortical local field potentials (LFP) or superficial EEG recordings.<sup>10,11</sup> Specifically, the fundamental cellular phenomenon underlying the EEG slow

waves of NREM sleep is the cortical slow oscillation.<sup>12-17</sup> The slow oscillation consists of an up state, characterized by sustained neuronal depolarization and irregular firing, which is followed by a hyperpolarized down state during which every cortical cell ceases firing due to disfacilitation. Simultaneous recordings of single-cell or multicellular activity and cortical LFPs under anesthesia and during physiologic sleep have revealed that sleep slow waves recorded with macroelectrodes are a reflection of near-synchronous transitions between up and down state in large populations of neurons.<sup>16,11,18</sup>

The homeostatic regulation of NREM SWA (from now on SWA) is a precise, ubiquitous, and basic feature of mammalian sleep.<sup>9</sup> The functional mechanisms underlying SWA regulation, however, are poorly understood. It was suggested recently that sleep SWA may reflect the average strength of cortical synapses, which would increase during wakefulness as a result of plastic processes and decrease during sleep due to a sleep-dependent mechanism of synaptic downscaling. Such synaptic homeostasis would restore brain efficiency with respect to energy consumption, neuropil density, cellular supplies, and potential for further plasticity.<sup>19,20</sup> The hypothesis maintains that high average synaptic strength facilitates network synchronization during sleep, which would appear in the EEG as increased SWA. The progressive decrease in SWA during sleep, on the other hand, would reflect a decrease in network synchronization due to the weakening of cortical connections.<sup>20,21</sup>

To explore the relationship between cortical synaptic strength and sleep SWA, Esser et al, in the first of 3 companion papers, employed a large-scale computer model of the sleeping thalamocortical system to simulate the cellular and network dynamics of cortical slow oscillations.<sup>22</sup> The model integrates detailed neuro-

## Disclosure Statement

This was not an industry supported study. The authors have indicated no financial conflicts of interest.

Submitted for publication December, 2006

Accepted for publication September, 2007

Address correspondence to: Giulio Tononi Department of Psychiatry, University of Wisconsin-Madison, 6001 Research Park Blvd, Madison, WI 53719; E-mail: gtononi@wisc.edu

nal properties with thalamocortical anatomy to reproduce sleep activity patterns at multiple levels, from intracellular membrane potentials to LFPs. These simulations showed that a net decrease in cortical synaptic strength leads to a reduced amplitude of cellular slow oscillations and to a marked decrease in network synchronization. In turn, these changes result in a reduction of SWA in the simulated LFP. During a given slow wave, recruitment is a measure of the number of neurons becoming active, whereas decruitment is a measure of the number of neurons becoming silent.<sup>22</sup> The simulations also show that reduced synaptic strength leads to decreased rates of neuronal recruitment and decruitment during the transition between the down and the up state of the slow oscillation. In turn, changes in neuronal recruitment/decruitment lead to characteristic changes in slow-wave parameters, including a decrease in the number of high-amplitude slow waves, a decrease in the slope of slow waves, and an increase in the number of multipeak waves.

The demonstration that the slope of sleep slow waves, which are evoked by spontaneously occurring volleys of neural activity, changes as a function of synaptic strength, is of particular interest because the slope of responses evoked by electrical stimulation is a well-established measure of synaptic efficacy. Specifically, it is known that the slope (time derivative) of population responses is proportional to the strength of the transmembrane currents underlying the generation of excitatory postsynaptic potentials.<sup>23</sup> Moreover, various experimental paradigms aimed at inducing changes in synaptic efficacy, such as tetanic stimulation and exploratory behavior (e.g.,<sup>24-27</sup>), produce reliable changes in the slope of evoked responses. Changes in response slope are also accompanied by changes in the number of synaptic glutamatergic AMPA receptors.<sup>28</sup>

In this paper, the predictions generated in the first companion paper<sup>22</sup> by large-scale computer simulations of sleep slow waves as a function of synaptic strength were examined by recording cortical slow waves in vivo using LFP electrodes in freely behaving rats. We focused on comparing slow-wave parameters in early sleep (at the beginning of the light period or after sleep deprivation), when the homeostatic sleep pressure is high, and in late sleep (at the end of the light period or at the end of recovery sleep after sleep deprivation), when the homeostatic sleep pressure is low. We found that, in line with the model's predictions, the decline of SWA during sleep is associated with a decreased proportion of large-amplitude slow waves, a decrease in the slope of slow waves, and an increase in the number of multipeak waves. In the following companion paper,<sup>29</sup> the results obtained here in the rat are extended to high-density EEG recordings in humans.

## MATERIALS AND METHODS

### Animals

Male WKY rats (Harlan, 11-12 weeks old at time of surgery) were maintained on a 12-h light:12-h dark cycle (lights on at 10:00), with ambient temperature kept constant at  $23^{\circ}\text{C} \pm 1^{\circ}\text{C}$ . Under deep (1.5%-2%) isoflurane anesthesia, rats were chronically implanted in the frontal cortex (B: +2-3 mm, L: 2-3 mm) with bipolar concentric LFP electrodes (outer electrode: length: 1.5 mm, diameter: 0.8 mm; inner electrode projection: 1 mm, diameter: 0.28 mm; PlasticsOne, Inc., Wallingford, CT) for chronic polysomnographic recordings. Electrodes were fixed to the skull

with dental cement, and their position after sacrifice was verified on cresyl-violet stained coronal sections. In all cases, the deep electrode was located within layer V, whereas the superficial electrode was in layers I-II. Two stainless-steel wires (diameter 0.4 mm) inserted into the neck muscles served to record the electromyogram (EMG).

Immediately after surgery, the animals were individually placed in transparent Plexiglas cages ( $36.5 \times 25 \times 46$  cm) and kept in sound-proof recording boxes for the duration of the experiment. Seven to 10 days were allowed for recovery after surgery, and experiments were started only after the sleep/waking cycle had fully normalized. The rats were connected by means of a flexible cable to a commutator (Airflyte, Bayonne, NJ) and recorded continuously. To minimize the stress during sleep deprivation (see below), all animals were provided daily, at light onset, with a new paper towel and a novel object. Video recordings were performed continuously with infrared cameras (OptiView Technologies, Inc. Potomac Falls, VA) and stored in real time (AVerMedia Technologies, Inc. Milpitas, CA).

### LFP Recordings and Scoring of Behavioral States

All rats ( $n = 15$ ) were recorded during an undisturbed baseline period of 24 hours. LFP and the EMG signals were amplified (amplification factor 2000) and filtered (attenuation 50% amplitude [-6 dB]) as follows: LFP: high-pass filter at 0.1 Hz; low-pass filter at 30 Hz; EMG: high-pass filter at 10 Hz; low-pass filter at 100 Hz. All signals were sampled and stored at 128-Hz resolution. EEG power spectra were computed by a fast Fourier transform routine for 4-second epochs (0.25-Hz resolution).

NREM sleep, REM sleep, and wakefulness were scored off line in 4-second epochs by visual inspection of the LFP and EMG recordings. Wakefulness was characterized by a low-voltage, high-frequency LFP pattern and phasic EMG activity. NREM sleep was characterized by the occurrence of high-amplitude slow waves, spindles, and low tonic EMG activity. During REM sleep, cortical LFP was similar to that during waking, but only heart beats and occasional twitches were evident in the EMG signal. Epochs containing artifacts, predominantly during active wakefulness, were excluded from spectral analysis. Vigilance state could always be determined.

### Sleep Deprivation

To distinguish between circadian and sleep-wake dependent effects, a subgroup of rats ( $n = 7$ ) was sleep deprived for 6 hours, followed by an undisturbed recovery period. Sleep deprivation began at light onset and involved continuous observation of the animal and its polysomnographic recording. When the animal assumed a sleep posture, or started exhibiting electrographic signs of drowsiness, e.g., slow waves or low-tone EMG, it was given a novel object with which to play or was activated by acoustic stimuli (e.g., tapping on the cage). The animals were not touched or handled directly. The objects included paper tissue and paper towels, bedding material transferred from other cages, and toys of various shape and size. The rats were never disturbed when they were spontaneously awake, feeding, or drinking. Animal protocols followed the National Institutes of Health Guide for the Care and Use of Laboratory Animals and were in accordance with institutional guidelines.

## Detection and Analysis of Slow Waves

Detection of individual slow waves was performed on the LFP signal after band pass filtering (0.5–4 Hz, stopband edge frequencies 0.1–10 Hz) with MATLAB `filtfilt` function exploiting a Chebyshev Type II filter design (MATLAB, The Math Works, Inc., Natick, MA).<sup>13</sup> Filter settings were optimized visually to obtain the maximal resolution of wave shape, as well as the least intrusion of fast (e.g. spindle) activities (see Figure 2).

Slow waves were detected as positive deflections of the LFP signal between 2 consecutive negative deflections below the zero-crossing separated by at least 0.1 seconds (detection based on zero-crossings gave similar results). The first segment of the slow wave (from the first negative peak to the maximal positive peak) is thought to correspond to the down phase of the slow oscillations, whereas the second segment (from the maximal positive peak to the second negative peak) corresponds to the up phase.<sup>12–15, 17, 30</sup> This notion is supported by our observation of increased activity in the spindle frequency during and after the second segment of the slow wave (Supplementary Figure 1). The peak-to-peak amplitude of the first and second segment of the wave, the slopes (mean first derivative of the first and second segment), and the number of peaks within a single wave were computed for each individual wave during NREM sleep. Multipeak waves were defined as waves with more than 1 positive peak between 2 consecutive negative deflections below the zero crossing. To prove that multipeak waves are not merely a reflection of spindles or other high-frequency oscillations unrelated to slow waves, we normalized the number of peaks in multipeak waves to the corresponding wave duration. This computation revealed that there were, on average,  $3.65 \pm 0.03$  peaks per 1 second, indicating that the peaks are not the result of contamination by sleep spindles that occur at frequencies above 10 Hz.

All slow waves were sorted into 5 amplitude percentage ranges (20 percentiles each) according to the amplitude of the peak (from zero-crossing to maximum positive value), and all the parameters of individual slow waves were computed for each amplitude percentage range. To investigate whether the slopes of the slow waves in early and late sleep differ regardless of corresponding SWA and slow-wave amplitude, 4-second epochs for early and late sleep were matched by SWA and amplitude of the largest slow wave within the epoch (maximum allowable difference  $\pm 5\%$  for either parameter). The relative difference (% of mean) of the slopes of the slow waves for each match (mean number of comparisons  $1148.7 \pm 49.5$ ,  $n = 15$ ) was then computed and averaged for each rat prior to computing group means.

To account for a potential effect of slow-wave period on the computation of the slope, we also considered the maximal instantaneous slope of the first and second segment, which was computed as the maximal value of their first derivative.

## Simulating the LFP Signal in Early and Late Sleep

To investigate how changes in the power spectrum in the SWA range are related to changes in slow-wave parameters, we created artificial LFP signals corresponding to early and late sleep. We created a time series made up of individual waves based on the average LFP slow wave, with either 1 peak (peak-to-peak amplitude 2.0 mV) or 2 peaks (amplitude 1.7 mV), inserted at random intervals (Gaussian distribution with mean  $\sim 1$  sec) on a back-

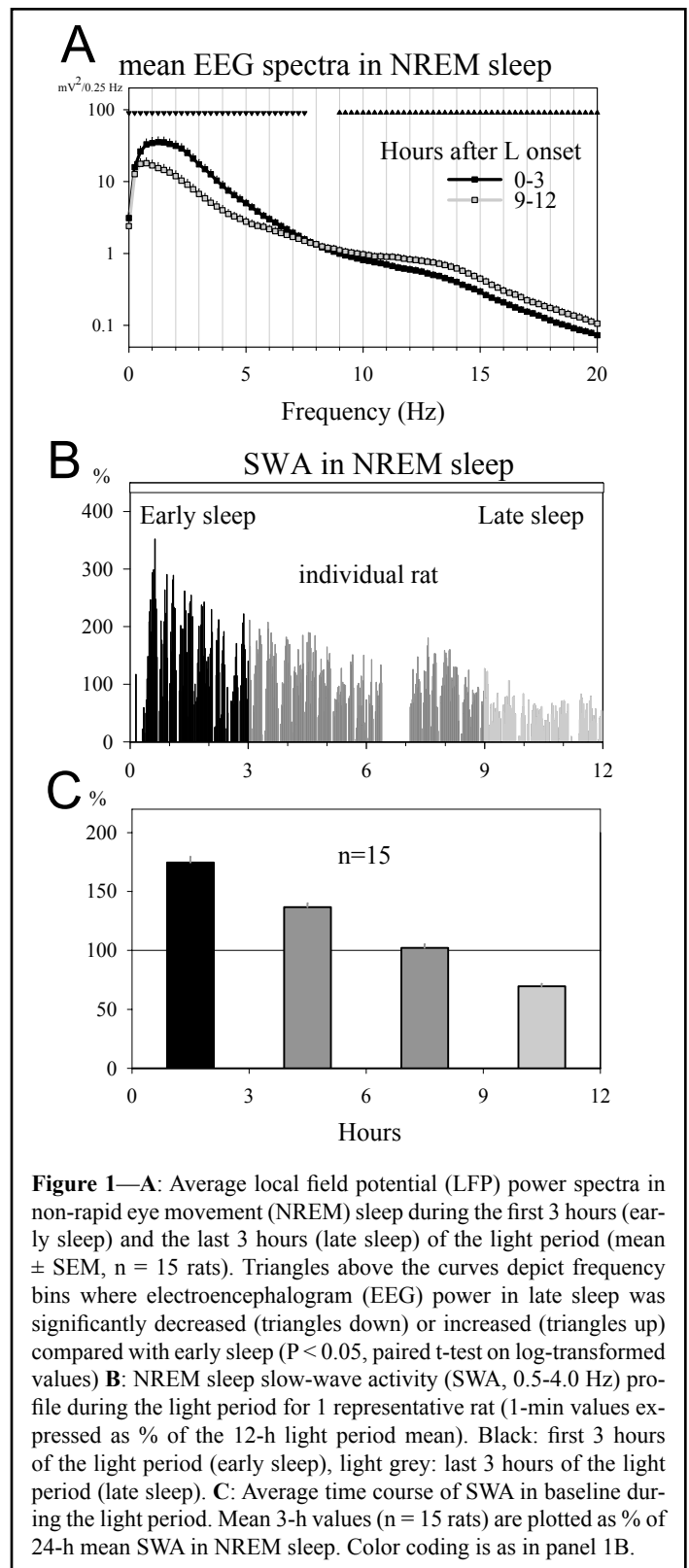


**Figure 1—A:** Average local field potential (LFP) power spectra in non-rapid eye movement (NREM) sleep during the first 3 hours (early sleep) and the last 3 hours (late sleep) of the light period (mean  $\pm$  SEM,  $n = 15$  rats). Triangles above the curves depict frequency bins where electroencephalogram (EEG) power in late sleep was significantly decreased (triangles down) or increased (triangles up) compared with early sleep ( $P < 0.05$ , paired t-test on log-transformed values). **B:** NREM sleep slow-wave activity (SWA, 0.5–4.0 Hz) profile during the light period for 1 representative rat (1-min values expressed as % of the 12-h light period mean). Black: first 3 hours of the light period (early sleep), light grey: last 3 hours of the light period (late sleep). **C:** Average time course of SWA in baseline during the light period. Mean 3-h values ( $n = 15$  rats) are plotted as % of 24-h mean SWA in NREM sleep. Color coding is as in panel 1B.

ground of pink noise (scaled to 1 mV and synthesized by inverse discrete Fourier transform of a vector of logarithmically decreasing power values). In this way, we approximated the  $1/f$  distribution of spectral power for the real LFP signal (Figure 1).

Three parameters of the artificial signal were varied to simulate early and late sleep conditions. (1) The redistribution of slow-wave amplitudes was simulated by decreasing by 80% the amplitude of 6 out of each 7 waves for the late sleep condition, compared with 1 out of 7 waves for the early sleep condition.

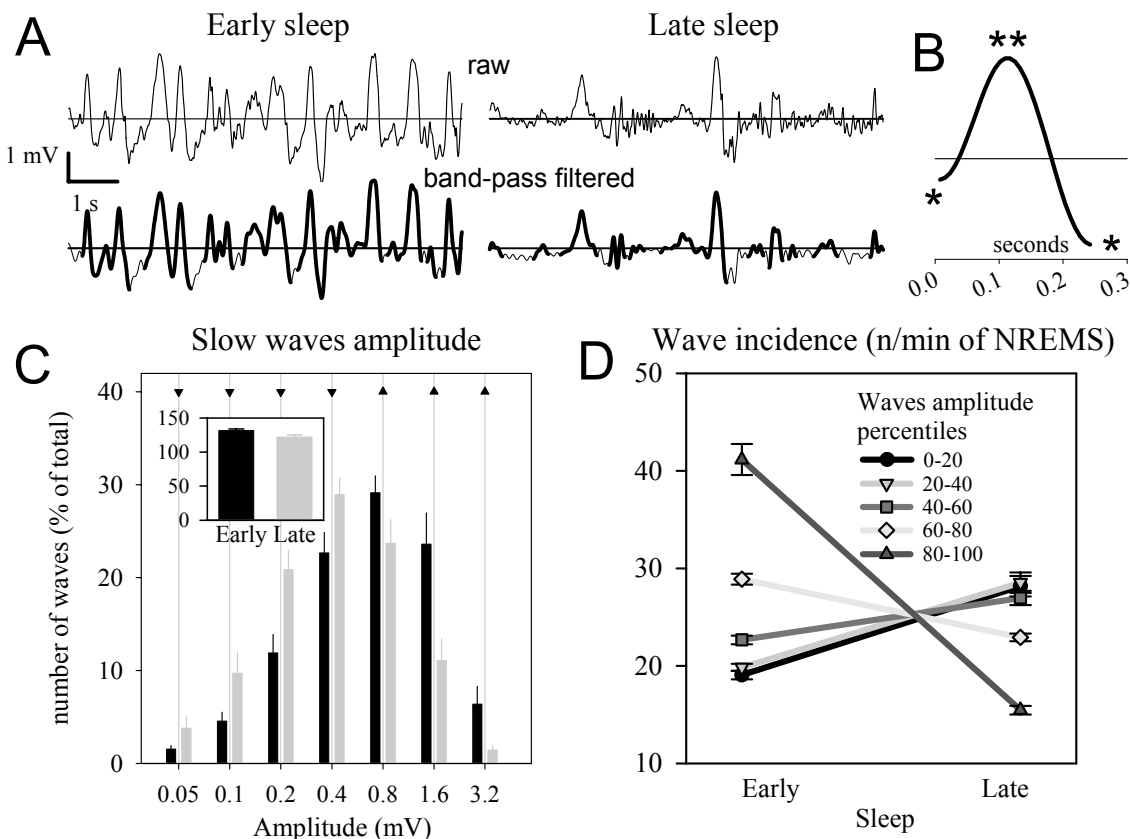


**Figure 2**—**A**, top traces: Representative raw local field potentials (LFP) during early and late sleep; bottom traces: corresponding band-pass filtered signal (0.5–4 Hz). The detected slow waves are highlighted. **B**: Representative individual slow wave detected by the algorithm. The first and second segment of the slow wave between the negative peaks (\*) and the positive peak (\*\*) are indicated. **C**: Distribution of the amplitude of the slow waves during early and late sleep. The number of waves was computed for groups with logarithmically increasing amplitude. Mean values ( $\pm$  SEM,  $n = 15$  rats) are plotted as percentage of the total number of waves (13 rats still had slow waves in late sleep  $> 1.6$  mV). The inset shows the mean incidence (number of waves/min of non-rapid eye movement sleep [NREMS]). The number is only  $8.0\% \pm 0.2\%$  lower in late vs early sleep. Triangles above the bars denote amplitude ranges in which slow-wave incidence was higher during early sleep (triangles up) or higher during late sleep (triangles down,  $P < 0.05$ , Sidak test). **D**: Slow-wave incidence during early and late sleep. All slow waves for each rat ( $n = 15$ ) were subdivided into 5 equal amplitude ranges (20 percentiles each) based on the amplitude of the peak (see Materials and Methods). The wave incidence changed significantly in all ranges of amplitude ( $P < 0.01$ , paired t-test).

(2) The decrease of the slope of the slow waves in the late sleep condition was simulated by prolonging the duration of all waves by approximately 33% while keeping the amplitude constant. (3) The increased proportion of multipeak waves in the late sleep condition was simulated by inserting a double peak every third wave, compared with 1 out of every 4 waves for the early sleep condition. In addition, in order to assess the contribution of each parameter to the resulting power spectrum, we created signals in which either only the proportion of high-amplitude waves or only slow-wave slopes were varied, and the resulting power spectra were compared. The simulations were performed repeatedly to ensure reproducibility of the results. Average spectra were computed over 60 minutes of simulated LFP.

### Statistical Analysis

The effects of homeostatic sleep pressure (early sleep vs late sleep) on the distribution of wave amplitude were assessed by the Sidak test, which provides adjusted P-values for multiple independent paired comparisons. The effects of homeostatic sleep pressure and amplitude percentage range on slow-wave parameters were assessed by analyses of variance (ANOVA) for re-

peated measures and subsequent paired t-tests (significance level adjusted for multiple comparisons by Bonferroni correction). The effects of sleep deprivation were analyzed by 2-way rANOVAs with factors “day” (baseline, recovery), and “time interval.” Linear regression analysis by the method of least squares was used to identify linear relationships between SWA and several wave parameters.

### RESULTS

In this study, we used the EEG signals derived from intracortical LFPs to investigate how homeostatic changes in SWA are reflected in changes in the morphology of the slow waves during NREM sleep. Superficial EEG signals from screw electrodes placed a few millimeters apart have previously been used in period-amplitude analysis studies.<sup>31,32</sup> However, signals from superficial recordings may cancel out or alter the shape of waves that are present synchronously in neighboring locations (Vyazovskiy et al, unpublished observation). This problem does not exist with intracortical LFPs because they sample deep and superficial layers within the same cortical column. As expected, referential recordings performed separately from the deep and the superficial

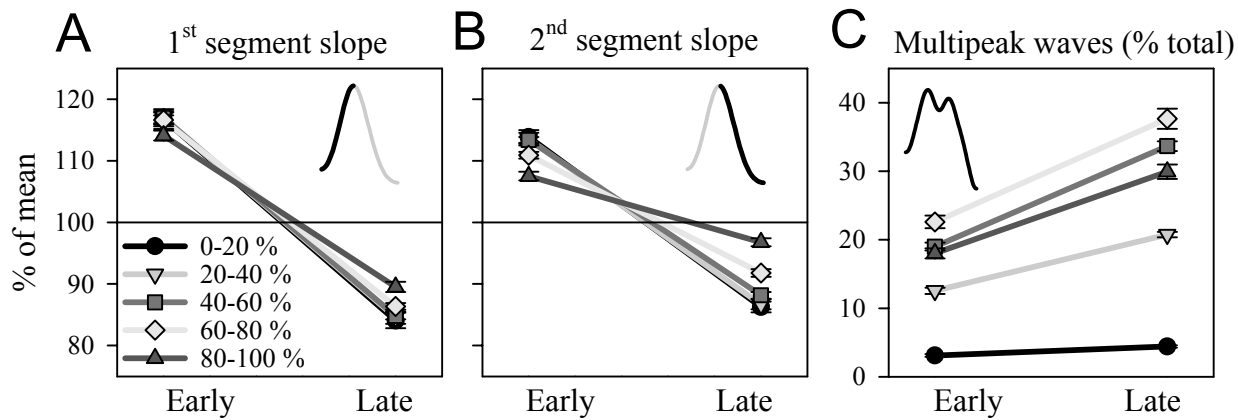


**Figure 3—A, B:** Slope of the first and second segment of the slow waves in early and late sleep. Slow waves were subdivided into 5 amplitude percentage ranges (20 percentiles each) according to the amplitude of the peak, and mean values ( $n = 15$  rats) are expressed as % of the 12-h mean. Corresponding mean values of the slopes (shown as = 100%) for the five amplitude percentage ranges were ( $\text{mV}/1 \text{ s}$ ): first segment:  $2.0 \pm 0.2$ ,  $2.5 \pm 0.2$ ,  $3.3 \pm 0.3$ ,  $4.6 \pm 0.5$ ,  $7.5 \pm 0.7$ ; second segment:  $1.9 \pm 0.2$ ,  $2.6 \pm 0.3$ ,  $3.7 \pm 0.4$ ,  $5.7 \pm 0.6$ ,  $9.7 \pm 0.9$ . **C:** Number of slow waves with more than 1 peak, expressed as percentage of the total number of waves during early and late sleep.

electrode relative to the cerebellum revealed opposite polarity of the slow wave (deep: positive; surface: negative), with a larger contribution of the deep electrode.

Conventional behavioral state scoring was initially performed using both surface and LFP recordings. Since the results were identical, all subsequent scoring was performed on the LFP signal. During baseline, all rats showed a strong diurnal preference for sleep during the light period ( $n = 15$ , mean in hours  $\pm$  SEM; waking  $2.8 \pm 0.1$ , NREM sleep  $7.3 \pm 0.09$ , REM sleep  $1.9 \pm 0.05$ ) relative to the dark period (waking  $8.0 \pm 0.2$ , NREM sleep  $3.4 \pm 0.2$ , REM sleep  $0.4 \text{ h} \pm 0.04$ ; light vs dark,  $P < 0.001$  for each vigilance state, paired t-test).

### LFP Signals Show a Progressive Decline of SWA from Early Sleep to Late Sleep

As expected, during NREM sleep, the LFP power in the slow-wave range showed a pronounced decline across the light period (Figure 1A;  $P < 0.001$ , 1-way rANOVA, factor “time interval”). SWA (0.5–4.0 Hz, Figure 1B,C) peaked at light onset ( $174.6\% \pm 5.2\%$  of 24-h mean) and declined afterward, reaching the lowest values during the last 3 hours of the light period ( $69.7\% \pm 2.0\%$  of 24-h mean). This decline was specific for the low frequencies ( $< 7.5 \text{ Hz}$ , paired t-test on log-transformed spectral values). In addition to the overall decline of EEG power from early to late sleep, a shift toward lower frequencies was apparent (see below and Figure 7).

### Late Sleep is Associated with Decreased Incidence of High-amplitude Slow Waves, Decreased Wave Slopes, and a Higher Proportion of Multipeak Waves

To investigate various parameters of slow waves, LFP signals were analyzed in the time domain and compared between early sleep and late sleep. “Early sleep” refers to the sleep epochs during the first 3 hours of the light period, whereas the last 3 hours before lights off are referred to as “late sleep.” Figure 2A shows examples of the detection of slow waves in these 2 conditions. Single slow waves were detected on the band-pass filtered signal (0.5–4 Hz) as positive deflections between 2 consecutive negative

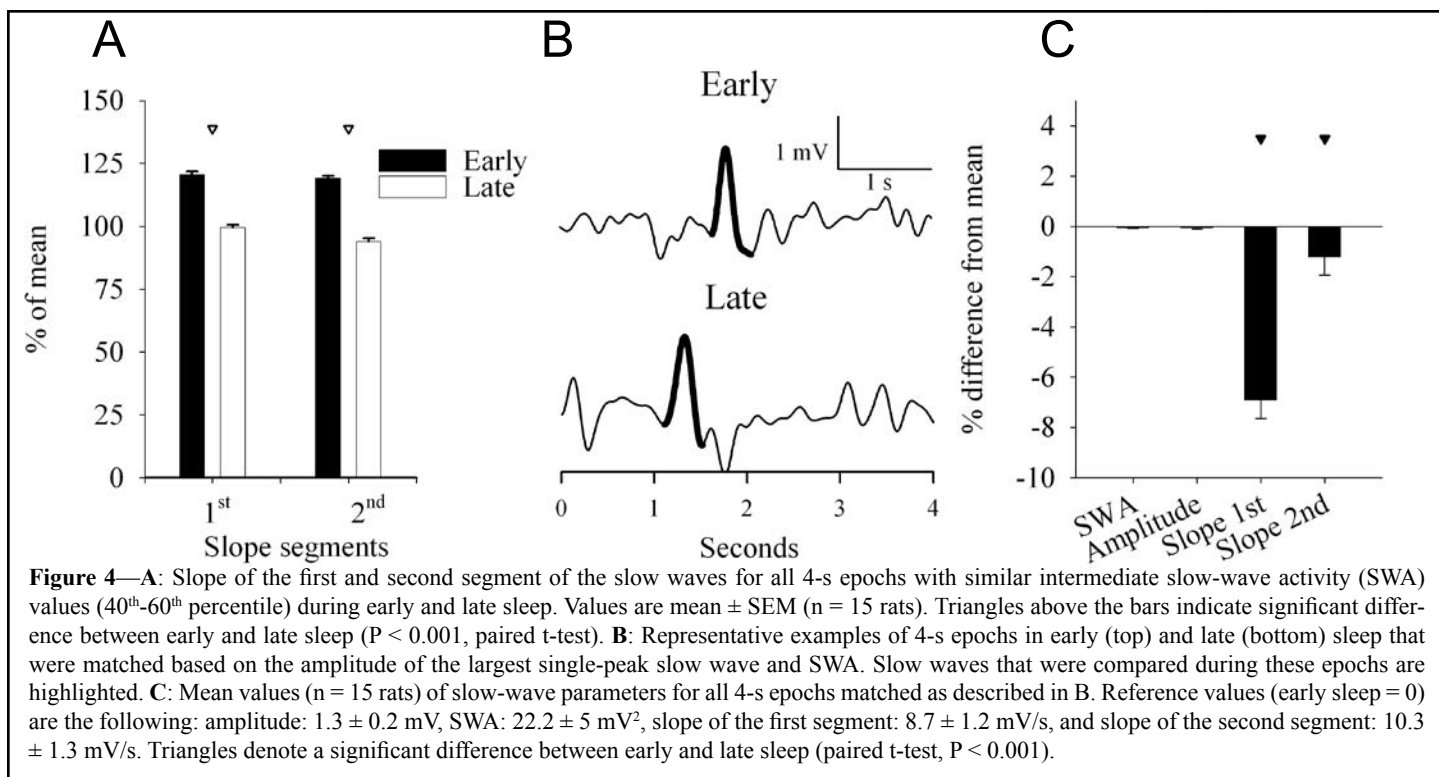
peaks (negative peaks: downward deflections  $< 0$ , Figure 2B; see Materials and Methods for details).

### Wave Incidence and Amplitude

The total number of slow waves detected did not change markedly between early and late sleep (Figure 2C inset). By contrast, the 2 conditions differed significantly in the relative proportion of slow waves of high and low amplitude (Figure 2C). Thus, concurrently with decreasing homeostatic sleep pressure during the light period, the number of high-amplitude slow waves decreased, whereas the number of low-amplitude waves increased. The change in wave incidence was significant for all 5 amplitude percentage ranges (Figure 2D; paired t-test after significance in ANOVA, factors “sleep pressure”  $\times$  “amplitude percentage range”,  $P < 0.001$ ). In late sleep, slow waves of the highest amplitude category (range 80%–100%) were still present in all rats ( $n = 15$ ) but were less abundant (see individual examples and histogram in Figure 2; range of number of waves across animals: early sleep, 3033–5828; late sleep: 1056–1938). Moreover, the largest waves in late sleep were just as large as the largest waves in early sleep; on average, only 0.73% of waves (range: 0.06%–2.8%) during the first 3 hours of the light period exceeded the largest wave during the last 3-hour interval.

### Wave Slopes

As shown in the representative example of Figure 2B, the average absolute amplitude of the first segment of the waves was lower compared with the second segment ( $0.7 \pm 0.1$  vs  $0.8 \pm 0.1 \text{ mV}$ ,  $P < 0.001$ , paired t-test), and the slope (the mean first derivative) of the second segment was steeper ( $3.8 \pm 0.4$  vs  $4.5 \pm 0.4 \text{ mV/s}$ ,  $P < 0.001$ , paired t-test). When considering all slow waves, the slope of both the first and the second segment was approximately 35% lower in late sleep compared to early sleep (Figure 3A,B; paired-test,  $P < 0.001$  after significant ANOVA). High-amplitude slow waves showed the most pronounced decrease in the slope of the first segment and the smallest change in the slope of the second segment (rANOVA, interaction factors “sleep pressure: high, low”  $\times$  “amplitude percentage range”,  $P < 0.001$ ).



To account for a potential effect of slow-wave period on the computation of the slope, we also considered the maximal instantaneous slope of the first and second segment that was computed as the maximal value of their first derivative. In this way, the duration of the wave did not directly enter the computation. We found that, in late sleep, the instantaneous slope of the first and second segment decreased to  $62.0\% \pm 1.5\%$  and  $63.9\% \pm 1.6\%$ , respectively, compared with early sleep ( $= 100\%$ ).

### Multipeak Waves

Another striking difference between early sleep and late sleep was the increased occurrence of waves exhibiting more than 1 peak (Figure 3C). On average, 1.2 peaks per slow wave occurred in early sleep, whereas, in late sleep, slow waves had, on average, 1.4 peaks ( $P < 0.001$ , paired t-test). The increase in the proportion of multipeak waves was significant for all 5 amplitude percentage ranges (paired t-test, corrected for multiple comparison after significant rANOVA, factor “sleep pressure: high, low” and interaction factors “sleep: early, late”  $\times$  “amplitude percentage range”,  $P < 0.001$ ).

### Slow-Wave Slopes are Steeper in Early Sleep than in Late Sleep Even for Epochs Equated for SWA and Wave Amplitude

Although early sleep was associated, on average, with a high proportion of high-amplitude slow waves and late sleep with a high proportion of low amplitude slow waves, we could identify individual epochs in early sleep with few or no large-amplitude waves, as well as epochs in late sleep with occasional high-amplitude waves. Typically, such epochs were nearly indistinguishable and could not be assigned correctly to early or high sleep condition based on visual inspection. Moreover, when examined in the frequency domain, we found that such visually indistinguishable epochs also had similar values of SWA.

We therefore asked whether the slope of the slow waves would reflect homeostatic sleep pressure even when SWA values and wave amplitude were comparable. To investigate this possibility, we employed 2 complementary strategies. First, all 4-second epochs in NREM sleep were subdivided into 5 percentage ranges as a function of their SWA value. Figure 4A illustrates the intermediate range ( $40^{\text{th}}\text{--}60^{\text{th}}$  percentile) and shows that the slope of the first and second segment was consistently steeper in early sleep compared with during late sleep (paired t-test after significant ANOVA, “sleep pressure” or “percentage range”  $\times$  “sleep pressure”,  $P < 0.001$ ). This difference was present in all 5 percentage ranges (not shown).

In the second approach (Figure 4B,C), 4-second epochs in early and late sleep were matched based on both SWA and the amplitude of the largest single-peak slow wave within the epochs. Subsequently, a difference was computed between corresponding slopes within each such pair of slow waves (on average,  $1148.7 \pm 49.5$  comparisons,  $n = 15$ ). Individual examples of slow waves that were compared in early and late sleep are illustrated on Figure 4B. Again, we found that the slopes of both the first and the second segment were consistently steeper in early sleep (Figure 4C;  $P < 0.001$ , paired t-test). Similar changes were also observed when the comparison was performed over all waves, including multipeak waves (not shown), and when slow waves were detected based on zero-crossings (not shown), as in the companion paper that used human high-density EEG data.<sup>29</sup>

### SWA and Slow-Wave Parameters Change Across Time in a Highly Correlated Manner

We measured SWA and slow-wave parameter values for 4 consecutive 3-hour intervals during the light period. The level of SWA showed a highly significant positive linear relationship with the incidence of high-amplitude slow waves (Figure 5A). Low-amplitude slow waves exhibited a negative relationship with

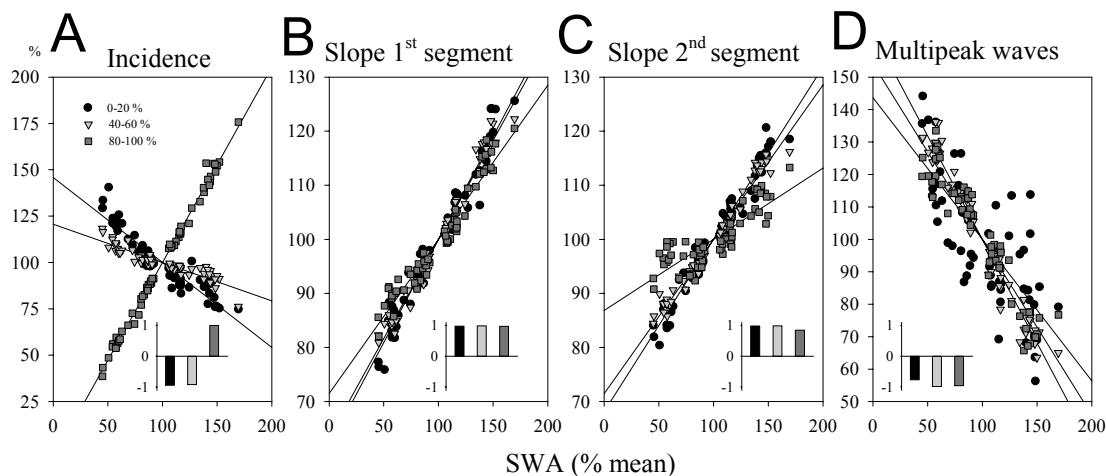


**Figure 5**—Relationship between non-rapid eye movement slow-wave activity (SWA) (0.5–4.0 Hz, % of 12-h light-period mean) and slow-wave parameters (incidence, slopes, multippeak waves, % of 12-h light-period mean) computed for the four 3-h intervals of the light period. All waves were subdivided into 5 amplitude percentage ranges based on the amplitude of the peak. Three-hour averages of the 0–20<sup>th</sup>, 40<sup>th</sup>–60<sup>th</sup> and 80<sup>th</sup>–100<sup>th</sup> amplitude percentiles are shown. Lines depict linear regression. Insets: significant *r*-values of the Pearson correlation (all: *P* < 0.05).

the decrease of SWA, as expected given the mirror-image time course of high- and low-amplitude waves (Figure 2). A strong, highly significant positive correlation was also evident between the slopes of the first and second segment of the slow waves (for all 5 amplitude percentage ranges) and the level of SWA (Figure 5B,C). Finally, the proportion of multippeak waves was negatively correlated with SWA (Figure 5D).

### Slow-Wave Slopes Increase Further After Sleep Deprivation

Despite the strong correlation between the slow-wave parameters investigated here and the homeostatic changes in SWA, the possibility remains that the observed changes may also be related to circadian factors. To disentangle circadian from homeostatic effects, we performed 6 hours of sleep deprivation by gentle handling in a subset of animals (*n* = 7). Sleep deprivation was successful—only  $10.4 \pm 4.1$  minutes of NREM sleep occurred during the 6 hours (2.9 % of total time). As shown in Figure 6, compared with the corresponding baseline interval, the first 2 hours of recovery sleep after sleep deprivation were associated with an increased incidence of high-amplitude waves (Figure 6A), a steeper slope of the first and second segment (Figure 6C,D), and a decrease in the number of multippeak waves (Figure 6B). During the subsequent 6 hours of recovery sleep, slow-wave incidence and the slopes decreased, whereas the proportion of multippeak waves increased, approaching baseline levels (rANOVA, interaction factors “day: baseline, recovery”  $\times$  “time interval”, *P* < 0.001 for all 4 variables).

### Changes in EEG Spectra Between Early and Late Sleep can be Accounted for by Simulating the Observed Changes in Slow-Wave Parameters

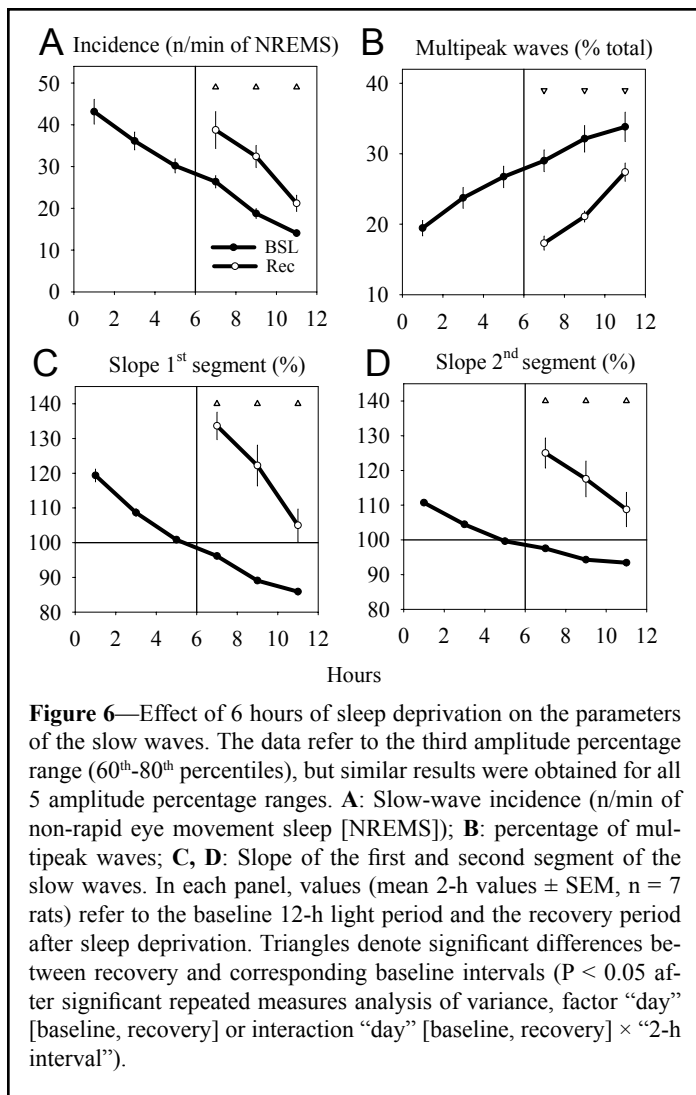
The power in the SWA range is ultimately related to synchronous oscillations of large populations of cortical neurons, which can be recorded as low-frequency LFP or superficial EEG recordings.<sup>11</sup> We therefore examined whether the changes in the distribution and morphology of slow waves reported here can account

for the well-established decline in SWA during the course of sleep. To do so, we generated an artificial signal that reproduced the main parameters of the LFP signal in the early and late sleep conditions (see Materials and Methods, Figure 7A). As shown in Figure 7B (lower panels), when we calculated the absolute power spectrum for the simulated “late-sleep” LFP, we found a marked decrease in the SWA range. In addition, the normalization of the spectra to the mean power between 0.5 and 4.0 Hz revealed a shift of the spectral peak to a lower frequency bin (0.75 vs 1.5 Hz). A similar shift in the relative spectrum was observed in vivo when we compared the LFP signals between the early and the late sleep conditions (Figure 7B, upper panels).

We then manipulated the various slow-wave parameters independently to evaluate their individual contribution to power spectral changes. A decreased proportion of high-amplitude slow waves resulted in overall lower spectral values in the low-frequency range (Figure 7C). In contrast, a decreased slope of slow waves resulted in a shift of spectral power towards lower frequencies (Figure 7D). Thus, this analysis suggests that the redistribution of high- and low-amplitude slow waves between the early and late sleep conditions is primarily responsible for the decrease in absolute power in the SWA range, whereas the reduced slope of slow waves in the low sleep pressure condition is responsible for the increase in the low-frequency power (< 1.5 Hz) at the expense of power above 1.5 Hz.

### DISCUSSION

We recorded rat cortical LFP during NREM sleep to measure the incidence and shape of sleep slow waves as a function of decreasing homeostatic sleep pressure. We found that, at the beginning of the major sleep phase or after sleep deprivation, when homeostatic sleep pressure and SWA are high, there are many large slow waves, the slope of the slow waves is steep, and multippeak waves are rare. By contrast, when homeostatic sleep pressure and SWA decline, large waves are few, the slope of slow waves decreases, and multippeak waves become frequent.



### Incidence of High-Amplitude Slow Waves

A consistent finding of this study was that, although the total number of slow waves during the light period remained roughly constant, the proportion of high-amplitude slow waves decreased from early to late sleep. Computer simulations in a companion paper<sup>22</sup> suggest that a net reduction of synaptic strength leads to a decreased proportion of slow waves of large amplitude in late sleep through the following 2 mechanisms: (1) a smaller amplitude of the slow oscillation of the membrane potential of individual neurons and (2) a poorer synchronization between neurons. It should be noted that, in our data, the largest waves detected in late sleep were just as large as the largest waves we could detect in early sleep. Unlike human scalp EEG data, bipolar intracortical LFP recordings are not affected by volume conduction, and reflect primarily local signals. Assuming that very large waves reflect a full recruitment of local neural populations (saturation), the present results suggest that full recruitment is possible both under high and low homeostatic sleep pressure, but it occurs much more rarely in the latter condition.

### Slow-Wave Slopes

A major finding of this study was the clear-cut decrease in the slope of slow waves with decreasing homeostatic sleep pressure.

Thus, the slopes of slow waves were steeper at the beginning of the light period and after sleep deprivation and decreased in the course of sleep.

As discussed in our companion paper,<sup>22</sup> changes in slope are of particular interest because they represent potential indicators of cortical synaptic strength. Indeed, in vitro and in vivo, in both cerebral cortex and hippocampus, long-term potentiation and long-term depression of synaptic transmission are characteristically associated with an increase and a decrease, respectively, in the slope of evoked potentials.<sup>26, 27, 33, 34</sup> Although the slow waves of NREM sleep studied here are spontaneous events, they are also to some extent “evoked” by spontaneous volleys of activity traveling within the cortex,<sup>35</sup> and, thus, it is reasonable to assume that their slope could reflect synaptic strength. This assumption is supported by recent experiments in our laboratory, where we measured the slope of transcallosal evoked responses in the rat cerebral cortex. Like the slope of the spontaneous slow waves studied here, the slope of cortical evoked responses triggered by electrical stimulation was steepest under naturally elevated homeostatic sleep pressure (at light onset or after sleep deprivation) and declined after undisturbed sleep.<sup>36</sup>

The computer simulations presented in our companion paper<sup>22</sup> indicate that changes in slow-wave slope as a function of synaptic strength are due to changes in the speed of recruitment/decruitment of neurons in the population slow oscillation. Specifically, the reduced slope of the second segment of the LFP slow wave is due to a decreased rate of recruitment of neurons into the up state (the steeper the slope, the quicker the recruitment), caused in turn by a reduced efficacy of cortical connections. Similarly, the slope of the first segment of the LFP slow wave, corresponding to the network’s transition into the down state, is reduced due to a decrease in the rate at which cells are decruited (the steeper the slope, the quicker the decruitment). The finding of a steeper slope of the second segment in our study is consistent with intracellular recordings showing faster rates of recruitment associated with a steeper transition into the up state (<sup>37, 38</sup>, but see <sup>39</sup>). In this context, it should be mentioned that previous studies employing period-amplitude analysis had demonstrated an increase in slow-wave period with decreasing sleep pressure,<sup>31, 32, 40</sup> and increased wave period usually entails decreased wave slope. Consistent with these earlier results, our data confirm a lengthening of wave period during late sleep (not shown). However, based on the mechanistic link between synaptic strength and wave slope provided by experimental work,<sup>24–27</sup> as well as by our computer simulations,<sup>22</sup> and in the absence of data suggesting changes in the intrinsic frequency of cellular oscillators (the slow oscillation is actually an irregular network phenomenon that arises from the bistability of cortical circuits<sup>41, 42</sup>), it seems more parsimonious to consider the change in wave period as a consequence of the change in wave slope, rather than the other way around.

### Multippeak Waves

Another finding of the present study was the increased occurrence of multippeak waves in the LFP signal in late sleep. According to our computer simulations,<sup>22</sup> multippeak LFP waves are due to the emergence of asynchronous spatially distinct clusters of activity, which are caused by poor spatial synchronization when the overall connection strength is reduced. This notion is supported



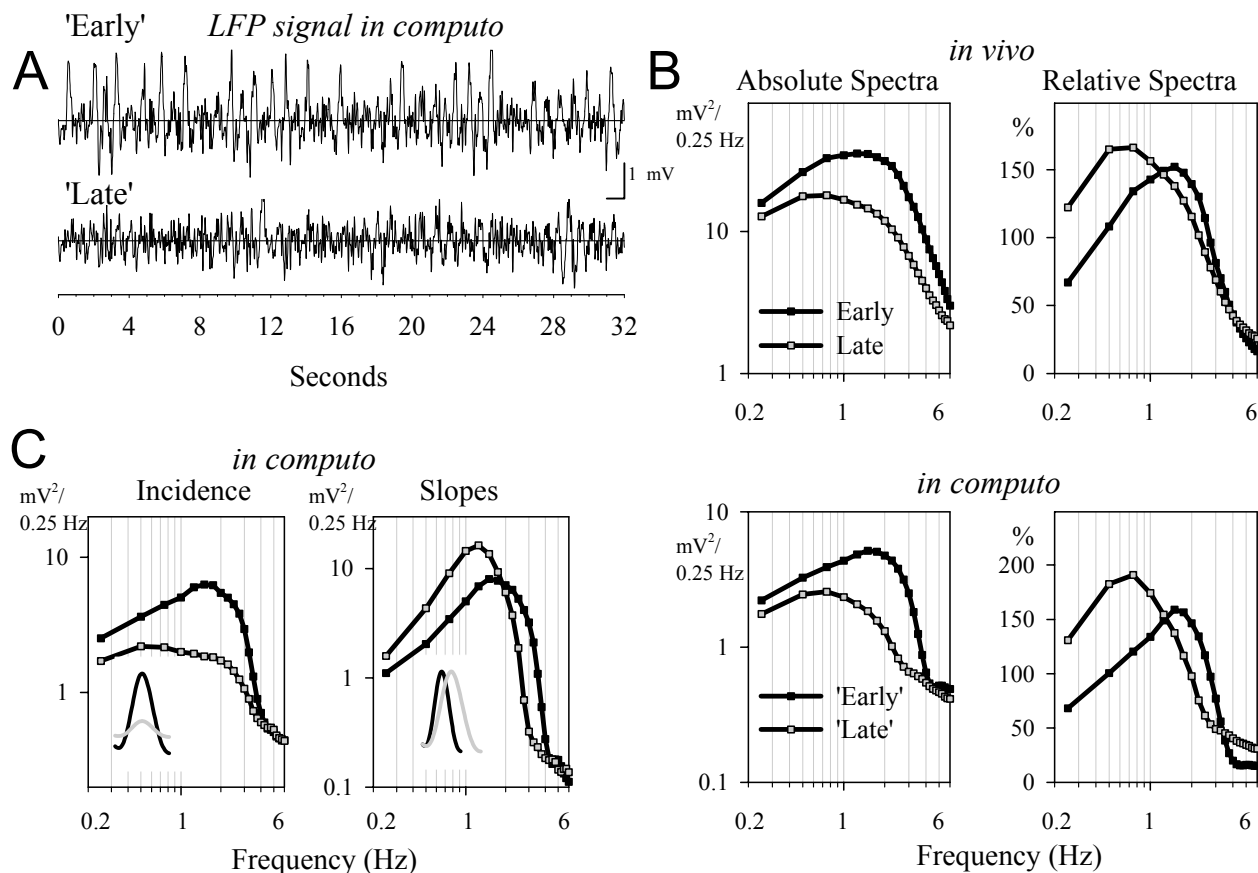


**Figure 7**—A: Representative traces of simulated local field potential (LFP) signal in the “early” and “late” sleep conditions (for comparison, an *in vivo* signal is shown in Figure 2A). B: Absolute and relative (% of mean power between 0.5–4.0 Hz) power spectra of the *in vivo* LFP signal in early and late sleep ( $n = 15$  rats, as in Figure 1A) and spectra of the simulated signals (60 min). C: Absolute spectra of simulated signals, in which incidence of high-amplitude slow waves and slow-wave slopes were varied independently (insets show representative waveforms from the simulated signals).

by the topographic analysis performed in the companion human study employing high-density EEG, which shows that multipeak waves reflect the asynchronous generation of slow waves in distant cortical sources.<sup>29</sup> This study also shows that in humans, just as in rats, such multipeak waves increase in number during late sleep.<sup>29</sup> Taken together, these data suggest that, in early sleep, when synaptic connections are strong, most neurons get recruited and recruited nearly simultaneously. In late sleep, by contrast, when synaptic connections are weak, the asynchronous involvement of distant areas in the same wave likely results in the occurrence of a slow wave with multiple peaks. It should be mentioned that it is unlikely that spindles contribute significantly to the occurrence of multipeak waves because the frequency of the peaks was within the SWA range ( $< 4$  Hz).

### Effects of Sleep Deprivation

The observed changes in slow-wave parameters could be due to homeostatic changes in sleep pressure, as is the case for SWA,<sup>2</sup> but circadian factors could have played a role. To address this issue, we performed 6 hours of sleep deprivation starting at light onset. We found that the slope of the slow waves (both first and second segments) at the beginning of recovery sleep was markedly steeper, compared with the corresponding time of the preceding baseline day, during which sleep was undisturbed. Thus, like

SWA, amplitudes and slopes of the slow waves reflect homeostatic sleep pressure rather than circadian time.

### Correlation Between Slow-Wave Parameters and SWA

SWA is considered a reliable measure of homeostatic sleep pressure because it increases after waking, decreases during sleep, and increases further after sleep deprivation (reviewed in<sup>1,9</sup>). Our data indicate that the well-established changes in SWA are associated with changes in several parameters of individual slow waves: a strong correlation was found between SWA and the incidence of slow waves of different amplitude (positive correlation with high-amplitude waves, negative with intermediate- and low-amplitude waves, Figure 5). This finding is consistent with the redistribution of slow waves with decreasing homeostatic sleep pressure. The slope of all slow waves, regardless of amplitude, also showed a strong positive correlation with SWA and, therefore, may represent another marker of homeostatic sleep pressure. In fact, the slow-wave slope may be even more sensitive than SWA, since we found that the slope was steeper in early sleep compared with late sleep even after the 2 conditions were matched for amplitude and SWA (Figure 4). Such increased sensitivity would be expected if the slope of the slow waves reflects a basic cellular phenomenon such as cortical synaptic strength.

## Effects of Slow-wave Parameters on SWA Spectra: Empiric Data and Simulations

How does the decrease of SWA relate to changes in slow-wave parameters? Traditionally, the homeostatic regulation of sleep is described by the time course of SWA, which reflects both frequency and amplitude content of the signal but does not take into account the heterogeneity of individual waves. To investigate how changes in slow-wave parameters, namely amplitude distribution and slope, account for the decrease in spectral power within the SWA band, we employed computer simulations. The results show that a decreased proportion of large slow waves leads to an overall decrease in all frequencies between 0.5 and 4.0 Hz. Intriguingly, they also show that a decrease in the slope of the slow waves leads to a shift of the peak of the relative spectrum towards slower frequencies ( $< 1.5$  Hz). This finding is relevant in view of the previously reported dissociation between the homeostatic behavior of frequencies below 1 Hz and the remaining SWA frequencies.<sup>13, 43-45</sup> Indeed, our data suggest that the slower homeostatic decline of EEG power below 1 Hz<sup>44</sup> may simply reflect a redistribution of power density due to concomitant changes in the slope of the slow waves, rather than represent a distinct neurophysiologic process subject to different regulatory mechanisms.

### Other Potential Mechanisms Able to Affect the Slope of Slow Waves

Despite the remarkable fit between the predictions of modeling studies<sup>22</sup> and the empiric observations reported here and elsewhere,<sup>36</sup> it should be emphasized that changes in synaptic strength may not be the only mechanism able to account for the observed results. There are several additional mechanisms that could play a role in affecting the size of slow waves. A first mechanism implies a change in the balance between excitatory and inhibitory neurotransmission, such as a reduction in inhibitory tone, since decreased inhibition can increase neuronal excitability and cause a more efficient recruitment of neurons. For example, large slow waves can be induced by manipulations that potentiate GABA transmission and thereby increase neuronal hyperpolarization.<sup>46</sup> Thus, smaller slow waves at the end of the sleep period could reflect lower GABAergic inhibition. However, we are not aware of any evidence suggesting that the strength of the GABAergic inhibitory tone changes during the course of sleep. Moreover, and most importantly, in vivo, in vitro, and in computo evidence indicates that the down state of the slow oscillation, which is the cellular basis for sleep slow waves, is the result of disfacilitation (i.e., a lack of synaptic input), rather than of active inhibition.<sup>18, 21, 47</sup> A second, somehow complementary mechanism, may involve the progressive build-up, in the course of sleep, of arousal-promoting neuromodulators. It has been shown that the selective activation of cholinergic and noradrenergic cortical projections can block the cyclic hyperpolarization/depolarization components of the slow oscillations, resulting in the disappearance of slow waves and EEG activation.<sup>18</sup> Thus, if the activity of cholinergic, noradrenergic, histaminergic, or hypocretinergic neurons, or a combination thereof, were to increase in the course of sleep, the end result would be smaller slow waves and a decrease in SWA under low sleep pressure. So far, the available evidence does not support the hypothesis of a progressive accumulation of these neuromodulators in the course of the resting period (e.g.,<sup>48-50</sup>), although more direct data collected with higher temporal resolution

are needed. Similar studies to assess changes in cortical levels of glutamate are also needed because a progressive build-up of this excitatory neurotransmitter during sleep could also alter neuronal excitability. A third mechanism could include changes in the metabolic state of cortical neurons or glia cells, or in the levels of certain ions, or both—all factors that could globally affect neural excitability and, thus, the generation of slow waves. Although brain metabolism depends on behavioral state (e.g.,<sup>51</sup>), we are not aware of any evidence that it may change across the resting period independently of sleep and waking. Global changes in the levels of intracellular  $\text{Na}^+$ ,  $\text{Ca}^{++}$ , or  $\text{K}^+$  cannot be excluded a priori. However, they seem an unlikely candidate because intracellular ionic concentrations are strictly regulated, and direct evidence for their change in the course of sleep is presently lacking. A fourth mechanism could involve changes in the concentration of substances covarying with behavioral state, such as adenosine, which could also decrease neural excitability. In the cerebral cortex, adenosine levels reach a plateau after 5 hours of sleep deprivation and remain significantly elevated during the first 3 hours of recovery sleep, when the largest changes in SWA occur.<sup>52</sup> Thus, the available evidence does not seem to indicate that slow-wave changes can be directly related to changes in cortical levels of adenosine, but further studies in which adenosine is measured across the entire sleep period are needed to address this question.

It should be mentioned that, in theory, the relationship between the diurnal variations of slow-wave parameters and sleep SWA may have been confounded by brain temperature, which also shows pronounced daily change.<sup>53</sup> For instance, it has been shown in vitro that temperature changes of several degrees can change membrane input resistance and the size of action and after potentials by affecting  $\text{Ca}^{2+}$  and  $\text{K}^+$  conductances.<sup>54</sup> Temperature changes also affect the release probability of glutamate at neocortical synapses.<sup>55</sup> If the slope of the slow waves is determined by the rates of neuronal recruitment and decruitment,<sup>22</sup> which presumably depend on axonal conduction velocity, then the consequences of temperature could be significant. However, in our study, slow-wave parameters were compared between the first and the last 3 hours of the light period, when brain temperature is at a similar level (<sup>53, 56</sup> and our unpublished observations). Finally, it is important to mention that, in our study, the slopes of slow waves during early and late sleep were compared after having matched them for amplitude and SWA. This analysis showed that, in both rats (this study) and humans,<sup>29</sup> the slope of the slow waves was still steeper during early sleep relative to late sleep. In addition, slow waves of the highest amplitude occurred in late sleep, albeit at a lower rate.

### Concluding Remarks

The companion modeling study<sup>22</sup> showed that the homeostatic decrease of SWA in the course of sleep can be accounted for by a net decrease in the strength of cortical synapses. Moreover, the model predicted that the decrease in SWA as a function of synaptic strength should be accompanied by a decrease in the number of high-amplitude slow waves, a decrease in the slope of slow waves, and an increase in the number of multipeak waves. All these predictions were confirmed in detail in the present study of sleep slow waves in the freely behaving rat. Moreover, additional simulations based on rat LFP recordings showed that the observed change in slow-wave parameters fully explains the ho-

meostatic reduction of SWA in terms of power spectral analysis. Thus, a net change in cortical synaptic strength appears to provide a parsimonious account for the characteristic EEG changes that reflect changes in homeostatic sleep pressure.

A crucial role for changes in synaptic strength in determining changes in sleep SWA is also independently suggested by several observations, both in humans and in rats. For instance, (1) motor task learning produces a local increase in SWA<sup>35</sup>; (2) arm immobilization, which presumably produces synaptic depression in motor circuits, produces a local decrease in SWA<sup>57</sup>; (3) molecular markers of synaptic potentiation increase after waking and decrease after sleep, whereas markers of synaptic depression do the opposite<sup>58</sup>; and, finally, (4) the slope of cortical evoked potentials in freely behaving awake rats increases after a period of wakefulness and decreases after a period of sleep.<sup>36</sup> Taken together, these data support the hypothesis that the homeostatic changes of SWA during sleep can be accounted for by net synaptic potentiation during waking and net synaptic downscaling during sleep.<sup>19, 20</sup> Such regulation makes physiologic sense inasmuch as progressive strengthening of synapses cannot continue indefinitely because of constraints of energy, space, supplies,<sup>59</sup> and saturation of the ability to learn. Conceivably, the need for synaptic downscaling is triggered when synaptic crowding interferes with normal brain function and saturates the ability to learn. Indeed, there is compelling evidence that by triggering LTP-like mechanisms, learning can strengthen synapses to near the maximum of their modification range, impairing the further induction of LTP.<sup>60-62</sup> An intriguing possibility is that slow waves, which fall in a frequency range usually associated with depression, may not just reflect synaptic strength, but may actively contribute to the weakening of connections during sleep.<sup>19, 63</sup>

In summary, LFP recordings from the rat cerebral cortex demonstrate that several slow-wave parameters—the proportion of waves of large amplitude, the slope of individual slow waves, and the number of multipeak waves—change in parallel with the homeostatic decline of sleep SWA. As shown in a companion paper,<sup>22</sup> such changes in slow-wave parameters were predicted by computer simulations evaluating the effects of a hypothesized downscaling of cortical connections during sleep. In the next companion paper,<sup>29</sup> we examine whether the changes observed with rat LFPs can also be detected in human high-density EEG recordings.

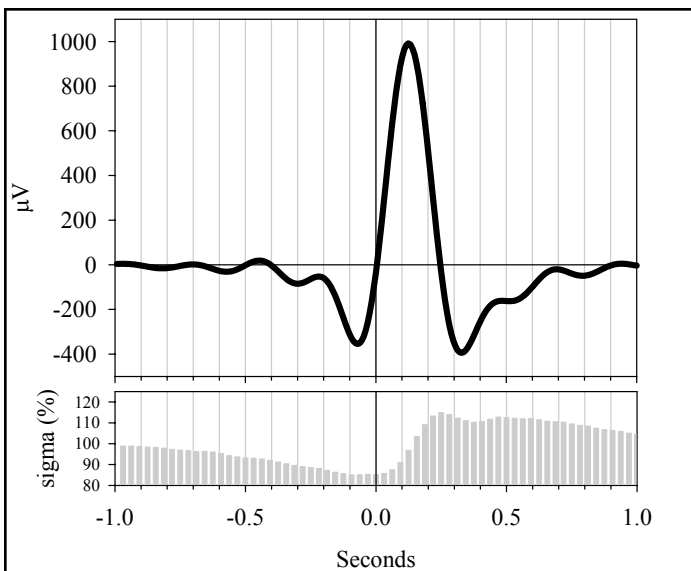
## ACKNOWLEDGMENT

We thank U. Faraguna for help with sleep deprivation. This research was supported by NIH Director's Pioneer Award to GT, Swiss National Science Foundation grant PBZHB-106264 to VVV, and NRSA T32 GM007507 and NIH T90 DK070079 to BAR.

## REFERENCES

- Borbély AA, Achermann P. Sleep homeostasis and models of sleep regulation. In Kryger MH, Roth T, Dement WC, eds. *Principles and practice of sleep medicine*. Philadelphia: Elsevier Inc, 2005. pp. 405-417.
- Borbély AA. A two process model of sleep regulation. *Hum Neurobiol* 1982;1:195-204.
- Daan S, Beersma DG, Borbely AA. Timing of human sleep: recovery process gated by a circadian pacemaker. *Am J Physiol* 1984;246: R161-83.
- Deboer T, Tobler I. Natural hypothermia and sleep deprivation: common effects on recovery sleep in the Djungarian hamster. *Am J Physiol* 1996;271:R1364-71.
- Huber R, Deboer T, Tobler I. Effects of sleep deprivation on sleep and sleep EEG in three mouse strains: empirical data and simulations. *Brain Res* 2000;857:8-19.
- Tobler I. Is sleep fundamentally different between mammalian species? *Behav Brain Res* 1995;69:35-41.
- Tobler I, Deboer T. Sleep in the blind mole rat *Spalax ehrenbergi*. *Sleep* 2001;24:147-54.
- Tobler I, Jaggi K. Sleep and EEG spectra in the Syrian hamster (*Mesocricetus auratus*) under baseline conditions and following sleep deprivation. *J Comp Physiol [A]* 1987;161:449-59.
- Tobler I. Phylogeny of sleep regulation. In Kryger MH, Roth T, Dement WC, eds. *Principles and practice of sleep medicine*. Philadelphia: Elsevier Inc, 2005. pp. 77-90.
- Nunez PL, Katznelson RD. *Electric fields of the brain: the neurophysics of EEG*. New York: Oxford University Press, 1981.
- Steriade M. Grouping of brain rhythms in corticothalamic systems. *Neuroscience* 2006;137:1087-106.
- Steriade M, Nunez A, Amzica F. A novel slow (< 1 Hz) oscillation of neocortical neurons in vivo: depolarizing and hyperpolarizing components. *J Neurosci* 1993;13:3252-65.
- Achermann P, Borbely AA. Low-frequency (< 1 Hz) oscillations in the human sleep electroencephalogram. *Neuroscience* 1997;81:213-22.
- Amzica F, Steriade M. Electrophysiological correlates of sleep delta waves. *Electroencephalogr Clin Neurophysiol* 1998;107:69-83.
- Destexhe A, Contreras D, Steriade M. Spatiotemporal analysis of local field potentials and unit discharges in cat cerebral cortex during natural wake and sleep states. *J Neurosci* 1999;19:4595-608.
- Steriade M, Timofeev I, Grenier F. Natural waking and sleep states: a view from inside neocortical neurons. *J Neurophysiol* 2001;85:1969-85.
- Steriade M, Amzica F. Slow sleep oscillation, rhythmic K-complexes, and their paroxysmal developments. *J Sleep Res* 1998;7 Suppl 1:30-5.
- Steriade M, Amzica F, Nunez A. Cholinergic and noradrenergic modulation of the slow (approximately 0.3 Hz) oscillation in neocortical cells. *J Neurophysiol* 1993;70:1385-400.
- Tononi G, Cirelli C. Sleep function and synaptic homeostasis. *Sleep Med Rev* 2006;10:49-62.
- Tononi G, Cirelli C. Sleep and synaptic homeostasis: a hypothesis. *Brain Res Bull* 2003;62:143-50.
- Hill S, Tononi G. Modeling sleep and wakefulness in the thalamocortical system. *J Neurophysiol* 2005;93:1671-98.
- Esser S, Hill S, Tononi G. Sleep homeostasis and cortical synchronization: I. Modeling the effects of synaptic strength on sleep slow waves. *Sleep* 2007;30:1617-30.
- Rall W. Distinguishing theoretical synaptic potentials computed for different soma-dendritic distributions of synaptic input. *J Neurophysiol* 1967;30:1138-68.
- Moser E, Mathiesen I, Andersen P. Association between brain temperature and dentate field potentials in exploring and swimming rats. *Science* 1993;259:1324-6.
- McNaughton BL, Barnes CA, Rao G, et al. Long-term enhancement of hippocampal synaptic transmission and the acquisition of spatial information. *J Neurosci* 1986;6:563-71.
- Bliss TV, Lomo T. Long-lasting potentiation of synaptic transmission in the dentate area of the anaesthetized rabbit following stimulation of the perforant path. *J Physiol* 1973;232:331-56.
- Glazewski S, Herman C, McKenna M, et al. Long-term potentiation in vivo in layers II/III of rat barrel cortex. *Neuropharmacology* 1998;37:581-92.
- Whitlock JR, Heynen AJ, Shuler MG, Bear MF. Learning induces long-term potentiation in the hippocampus. *Science* 2006;313:1093-7.

29. Riedner BA, Vyazovskiy VV, Huber R, et al. Sleep homeostasis, slow waves and cortical synchronization: III. A high-density EEG study of sleep slow waves in humans. *Sleep* 2007;30:1643-57.
30. Molle M, Marshall L, Gais S, Born J. Grouping of spindle activity during slow oscillations in human non-rapid eye movement sleep. *J Neurosci* 2002;22:10941-7.
31. Bergmann BM, Mistlberger RE, Rechtschaffen A. Period-amplitude analysis of rat electroencephalogram: stage and diurnal variations and effects of suprachiasmatic nuclei lesions. *Sleep* 1987;10:523-36.
32. Mistlberger R, Bergmann B, Rechtschaffen A. Period-amplitude analysis of rat electroencephalogram: effects of sleep deprivation and exercise. *Sleep* 1987;10:508-22.
33. Malenka RC. The long-term potential of LTP. *Nat Rev Neurosci* 2003;4:923-6.
34. Malenka RC, Bear MF. LTP and LTD: an embarrassment of riches. *Neuron* 2004;44:5-21.
35. Huber R, Ghilardi MF, Massimini M, Tononi G. Local sleep and learning. *Nature* 2004;430:78-81.
36. Vyazovskiy VV, Faraguna U, Cirelli C, Tononi G. Electrophysiological evidence for synaptic potentiation during waking and synaptic downscaling during sleep *Sleep* 2007;30(Abstract Supplement):A21-22.
37. Haider B, Duque A, Hasenstaub AR, McCormick DA. Neocortical network activity in vivo is generated through a dynamic balance of excitation and inhibition. *J Neurosci* 2006;26:4535-45.
38. Isomura Y, Sirota A, Ozen S, et al. Integration and Segregation of Activity in Entorhinal-Hippocampal Subregions by Neocortical Slow Oscillations. *Neuron* 2006;52:871-882.
39. Volgushev M, Chauvette S, Mukovski M, Timofeev I. Precise long-range synchronization of activity and silence in neocortical neurons during slow-wave oscillations [corrected]. *J Neurosci* 2006;26:5665-72.
40. Feinberg I, March JD, Fein G, et al. Period and amplitude analysis of 0.5-3 c/sec activity in NREM sleep of young adults. *Electroencephalogr Clin Neurophysiol* 1978;44:202-13.
41. Mukovski M, Chauvette S, Timofeev I, Volgushev M. Detection of Active and Silent States in Neocortical Neurons from the Field Potential Signal during Slow-Wave Sleep. *Cereb Cortex*. 2007 Feb;17(2):400-14.
42. Sanchez-Vives MV, McCormick DA. Cellular and network mechanisms of rhythmic recurrent activity in neocortex. *Nat Neurosci* 2000;3:1027-34.
43. Achermann P, Borbely AA. Temporal evolution of coherence and power in the human sleep electroencephalogram. *J Sleep Res* 1998;7 Suppl 1:36-41.
44. Campbell IG, Higgins LM, Darchia N, Feinberg I. Homeostatic behavior of fast Fourier transform power in very low frequency non-rapid eye movement human electroencephalogram. *Neuroscience* 2006;140:1395-9.
45. Dijk DJ, Beersma DG, Daan S. EEG power density during nap sleep: reflection of an hourglass measuring the duration of prior wakefulness. *J Biol Rhythms* 1987;2:207-19.
46. Vyazovskiy VV, Kopp C, Bosch G, Tobler I. The GABAA receptor agonist THIP alters the EEG in waking and sleep of mice. *Neuropharmacology* 2005;48:617-26.
47. Timofeev I, Grenier F, Steriade M. Disfacilitation and active inhibition in the neocortex during the natural sleep-wake cycle: an intracellular study. *Proc Natl Acad Sci U S A* 2001;98:1924-9.
48. Mitsushima D, Mizuno T, Kimura F. Age-related changes in diurnal acetylcholine release in the prefrontal cortex of male rats as measured by microdialysis. *Neuroscience* 1996;72:429-34.
49. Semba J, Toru M, Mataga N. Twenty-four hour rhythms of norepinephrine and serotonin in nucleus suprachiasmaticus, raphe nuclei, and locus coeruleus in the rat. *Sleep* 1984;7:211-8.
50. Yoshida Y, Fujiki N, Nakajima T, et al. Fluctuation of extracellular hypocretin-1 (orexin A) levels in the rat in relation to the light-dark cycle and sleep-wake activities. *Eur J Neurosci* 2001;14:1075-81.
51. Hofle N, Paus T, Reutens D, et al. Regional cerebral blood flow changes as a function of delta and spindle activity during slow wave sleep in humans. *J Neurosci* 1997;17:4800-8.
52. Porkka-Heiskanen T, Strecker RE, McCarley RW. Brain site-specificity of extracellular adenosine concentration changes during sleep deprivation and spontaneous sleep: an in vivo microdialysis study. *Neuroscience* 2000;99:507-17.
53. Franken P, Dijk DJ, Tobler I, Borbely AA. Sleep deprivation in rats: effects on EEG power spectra, vigilance states, and cortical temperature. *Am J Physiol* 1991;261:R198-208.
54. Thompson SM, Masukawa LM, Prince DA. Temperature dependence of intrinsic membrane properties and synaptic potentials in hippocampal CA1 neurons in vitro. *J Neurosci* 1985;5:817-24.
55. Volgushev M, Kudryashov I, Chistiakova M, et al. Probability of transmitter release at neocortical synapses at different temperatures. *J Neurophysiol* 2004;92:212-20.
56. Tobler I, Franken P, Gao B, et al. Sleep deprivation in the rat at different ambient temperatures: effect on sleep, EEG spectra and brain temperature. *Arch Ital Biol* 1994;132:39-52.
57. Huber R, Ghilardi MF, Massimini M, et al. Arm immobilization causes cortical plastic changes and locally decreases sleep slow wave activity. *Nat Neurosci* 2006;9:1169-76.
58. Pfister-Genskow M, Cirelli C, Tononi G. Molecular evidence for synaptic potentiation during waking and synaptic downscaling during sleep *Sleep* 2007;30(Abstract Supplement):A5-A6.
59. Attwell D, Laughlin SB. An energy budget for signaling in the grey matter of the brain. *J Cereb Blood Flow Metab* 2001;21:1133-45.
60. Foster TC, Gagne J, Massicotte G. Mechanism of altered synaptic strength due to experience: relation to long-term potentiation. *Brain Res* 1996;736:243-50.
61. Rioult-Pedotti MS, Friedman D, Donoghue JP. Learning-induced LTP in neocortex. *Science* 2000;290:533-6.
62. Sacchetti B, Lorenzini CA, Baldi E, et al. Time-dependent inhibition of hippocampal LTP in vitro following contextual fear conditioning in the rat. *Eur J Neurosci* 2002;15:143-50.
63. Czarnecki A, Birtoli B, Ulrich D. Cellular mechanisms of burst firing-mediated long-term depression in rat neocortical pyramidal cells. *J Physiol* 2007;578(Pt 2):471-9.



**Supplementary Figure 1**—Average high-amplitude slow wave (above median +1 SD of the positive peak amplitude), aligned to the first zero-crossing, and corresponding average profile of rectified signal after band-pass filtering between 10 and 15 Hz (sigma, bars: 1/32 s, % of mean longer than 2 s).